

## Thermodynamics of C-Mn-Si-Fe Quaternary Alloy

Tang Kai, Xu Jianlun, Ding Weizhong, Zhang Xiaobing, Jiang Guochang and Xu Kuangdi

Shanghai Enhanced Laboratory of Ferrometallurgy, Shanghai University  
149 Yanchang Road, Shanghai 200072, China

### Abstract

Based on the carbon solubility of Mn-Si-Fe alloys and the boundary conditions in sub-binaries and sub-ternaries, component activities of C-Mn-Si-Fe liquid quaternary alloys have been calculated by the new proposed solution model. The calculation results are in good agreement with the experiment data reported in the literature. The equilibrium relations associated with the production of manganese ferroalloys are also predicted and discussed in this paper.

### 1. Introduction

Ferromanganese and silicomanganese alloys are the main products of ferroalloy. These alloy systems can be described as C-Mn-Si-Fe quaternary melts. Thermodynamic properties of C-Mn-Si-Fe quaternary alloys are important to understand the equilibrium relations associated with the production of manganese ferroalloys. The general characteristic of ferroalloy melts is multicomponent and high concentration of solute. In order to predict the thermodynamic properties of ferroalloys, a solution model designed as SELF-SReM4.1 has been developed on the basis of sub-regular solution theory<sup>[1]</sup>. In this paper, the solution model is briefly introduced at first. Then, based on the carbon solubility data of C-Mn-Si-Fe quaternary melts and the thermodynamic properties in its sub-ternary and sub-binary systems, component activities of the C-Mn-Si-Fe quaternary alloy at 1873K have been predicted with the aid of the new proposed model. By combination of the alloy activities and the knowledge of distribution equilibria obtained in laboratory, reaction equilibrium between C-Mn-Si-Fe alloys and MnO-SiO<sub>2</sub>-CaO-Al<sub>2</sub>O<sub>3</sub> slags have been established.

### 2. The Solution Model

According to SELF-SReM4.1 model<sup>[1]</sup>, the isothermal excess partial Gibbs energy of four components in the homogeneity of a quaternary system can be expressed as polynomial function of composition variables,

$$\Delta G_1^E = \sum_{j=2}^i \sum_{k=0}^{j-1} \sum_{l=0}^{j-k} A_{jkl} Y^j Z^k W^l \quad (1)$$

$$\Delta G_2^E = \sum_{j=2}^i \frac{A_{j00}}{j-1} + \sum_{j=2}^i \sum_{k=0}^{j-1} \sum_{l=0}^{j-k} A_{jkl} Y^j Z^k W^l \left[ 1 + \frac{j-k}{Y(1-j)} \right] \quad (2)$$

$$\Delta G_3^E = \sum_{j=2}^i \sum_{k=0}^{j-1} \frac{A_{jk0}}{j-1} + \sum_{j=2}^i \sum_{k=0}^{j-1} \sum_{l=0}^{j-k} A_{jkl} Y^j Z^k W^l \left[ 1 + \frac{j-k}{Y(1-j)} + \frac{k-l}{YZ(1-j)} \right] \quad (3)$$

$$\Delta G_4^E = \sum_{j=2}^i \sum_{k=0}^{j-1} \sum_{l=0}^{j-k} \frac{A_{jkl}}{j-1} + \sum_{j=2}^i \sum_{k=0}^{j-1} \sum_{l=0}^{j-k} A_{jkl} Y^j Z^k W^l \left[ \frac{j-k}{Y(1-j)} + \frac{k-l}{YZ(1-j)} + \frac{l}{YZW(1-j)} \right] \quad (4)$$

and the isothermal excess integral Gibbs energy of quaternary system is written as,

$$\Delta G^E = \sum_{j=2}^i \frac{A_{j00}}{j-1} Y + \sum_{j=2}^i \sum_{k=1}^{j-1} \frac{A_{jk0}}{j-1} YZ + \sum_{j=2}^i \sum_{k=1}^{j-1} \sum_{l=1}^{j-k} \frac{A_{jkl}}{j-1} YZW + \sum_{j=2}^i \sum_{k=0}^{j-1} \sum_{l=0}^{j-k} \frac{A_{jkl}}{1-j} Y^j Z^k W^l \quad (5)$$

The composition variables chosen in the model are designated as  $Y$ ,  $Z$  and  $W$ . where,

$$Y = 1 - X_1 \quad (6)$$

$$Z = 1 - X_2 / Y \quad (7)$$

$$W = 1 - X_3 / YZ \quad (8)$$

$X_i$  ( $i=1, 2, 3, 4$ ) is the molar fraction of  $i$ th component.

$A_{jkl}$  are the parameters of the polynomials that can be evaluated along with the known "boundary conditions".  $j$ ,  $k$  and  $l$  are the upper limits of series that implicate the order of a given system. A special term "boundary condition" in the model can be defined as the measured thermodynamic properties in quaternary system, those in sub-ternaries and sub-binaries, the characteristic at the boundary of homogenous phase etc.

The temperature dependence of the thermodynamic properties may include in the parameters and is given by following equation,

$$A_{jkl} = \eta_{jkl} - \sigma_{jkl} T \quad (9)$$

where,  $\eta_{jkl}$  and  $\sigma_{jkl}$  are the temperature and composition inde-

Table 1. The Boundary Conditions in Binary Systems

System	Properties and Resource	Evaluation Formula	Reference
C-Mn(1-2)	$\Delta G_{Mn(C-Mn)}^E$ at 1623K, $\Delta G_{Mn(C-Mn)}^E$ at 1700K	$\Delta G_{Mn(C-Mn)}^E = \sum_{j=2}^j A_{j00} Y^j + \sum_{j=2}^j A_{j00} Y^j$	[6],[7]
C-Si(1-3)	hypothetical property obtained from C-Si-Fe	$\Delta G_{C(C-Si)}^E = \sum_{j=2}^j A_j^{13} Y^j = \sum_{j=2}^j \sum_{k=0}^{k'} A_{jk0} Y^j$	[4],[5]
C-Fe(1-4)	$\Delta G_{C(C-Fe)}^E$ at 1873K	$\Delta G_{C(C-Fe)}^E = \sum_{j=2}^j A_j^{14} Y^j = \sum_{j=2}^j \sum_{k=0}^{k'} \sum_{l=0}^{l'} A_{jkl} Y^j$	[8]
Mn-Si(2-3)	$\Delta G_{Mn(Mn-Si)}^E$ at 1873K	$G_{Mn(Mn-Si)}^E = \sum_{k=2}^{k'} A_k^{23} Z^k = \sum_{j=2}^j \sum_{k=0}^{k'} A_{jk0} \frac{k-1}{j-1} Z^k$	[5]
Mn-Fe(2-4)	$\Delta G_{Mn(Mn-Fe)}^E$ at 1863K	$G_{Mn(Mn-Fe)}^E = \sum_{k=2}^{k'} A_k^{24} Z^k = \sum_{j=2}^j \sum_{k=0}^{k'} \sum_{l=0}^{l'} A_{jkl} \frac{k-1}{j-1} Z^k$	[8]
Si-Fe(3-4)	$\Delta G_{Si(Si-Fe)}^E$ at 1873K	$\Delta G_{Si(Si-Fe)}^E = \sum_{l=2}^{l'} A_l^{34} W^l = \sum_{j=2}^j \sum_{k=0}^{k'} \sum_{l=0}^{l'} A_{jkl} \frac{l-1}{j-1} W^l$	[8]

pendent parameters. For the system the thermodynamic properties under deferent temperature is not available, following assumption is used to estimate the effect of temperature on the excess partial Gibbs energy of component *i*,

$$RT_1 \ln \gamma_i(T_1) = RT_2 \ln \gamma_i(T_2) \quad (10)$$

here,  $\gamma_i(T_1)$  and  $\gamma_i(T_2)$  are the *i*th component activity coefficients at temperature of  $T_1$  and  $T_2$  respectively.

When all parameters of quaternary system have been determined, activities of component *i* can be calculated by following equation,

$$a_i = \exp(\Delta G_i^E / RT) X_i \quad (i=1,2,3,4) \quad (11)$$

### 3. Parameters Evaluation Procedure

Measurements of the solubility of carbon in Mn-Si-Fe melts were carried out at temperature in the range of 1600-1900K by Petrushevskii *et al.*<sup>[2]</sup> and Tuset *et al.*<sup>[3]</sup> respectively. The result seems to be in fair agreement with each other. The relationship between C and Si contents in carbon saturated quaternary alloys with various Mn/Fe ratios at 1873K are shown in Figure 1.

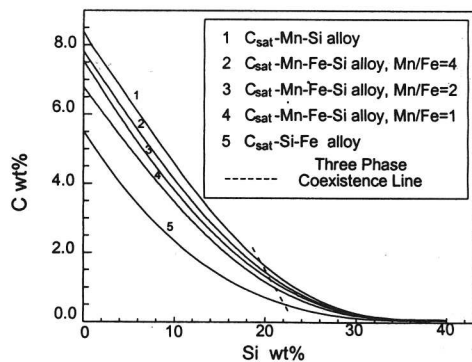


Figure 1. Solubility of Carbon in Mn-Si-Fe alloys at 1873K with various Mn/Fe ratios

Carbon solubility data of C-Mn-Si and C-Si-Fe alloys at same temperature, mainly based on the critical review of Ding<sup>[5]</sup> and the experimental results of Chipman and coworkers<sup>[4]</sup>, are also presented

in Figure 1. They can be used as ternary boundary conditions.

It is known from Figure 1 that either graphite or silicon carbide can coexist with the liquid alloys. For simplicity, the term “carbon saturated alloys” in the present paper will mean an alloy saturated either with graphite or SiC(β). At the lower silicon content range, the alloys equilibrate with graphite and the chemical potential of carbon in the alloys is constant. At high silicon content range, however, solid silicon carbide replaces the graphite as the stable phase. Then, the activity product of carbon and silicon remains constant defined by the equilibrium constant of following reaction,



where, the parentheses denote the metal phase. In the graphite/SiC(β)/alloy coexistence line of the carbon-saturated manganese alloys, carbon activity is unity regarding the solid graphite as the standard state. Thus, activity of silicon can be calculated from the equilibrium constant, at 1873K, is 0.033<sup>[5]</sup>, if activities of manganese, silicon and iron in the metal phase were chosen relative to pure liquid melts.

Denoting 1, 2, 3 and 4 as component C, Mn, Si and Fe respectively, then the excess partial Gibbs energy of components can be expressed as in the form of Eq(1) through Eq(4). Based on the information presented in Figure 1, we use following equations to describe the thermodynamic relations in C<sub>sat</sub>-Mn-Si-Fe quaternary alloys.

● When the alloys equilibrate with graphite, the chemical potential of carbon remains constant,

$$\Delta G_C^E = \sum_{j=2}^j \sum_{k=0}^{k'} \sum_{l=0}^{l'} A_{jkl} Y^j Z^k W^l = -RT \ln(1-Y) \quad (13)$$

● When the alloys saturated by SiC(β), the activity product of C and Si maintains constant,

$$\begin{aligned} \Delta G_C^E + \Delta G_{Si}^E &= \sum_{j=2}^j \sum_{k=0}^{k'} \frac{A_{jk0}}{j-1} \\ &+ \sum_{j=2}^j \sum_{k=0}^{k'} \sum_{l=0}^{l'} A_{jkl} Y^j Z^k W^l \left[ 2 + \frac{j-k}{Y(1-j)} + \frac{k-l}{YZ(1-j)} \right] \\ &= RT \ln K_{SiC} - RT \ln(1-Y) - RT \ln(YZ - YZW) \end{aligned} \quad (14)$$

● At the three phase coexistence line,

$$\Delta G_C^{E*} = \sum_{j=2}^j \sum_{k=0}^{k'} \sum_{l=0}^{l'} A_{jkl} Y^{*j} Z^{*k} W^{*l} = RT \ln a_C^* - RT \ln(1 - Y^*) \quad (15)$$

$$\Delta G_{Si}^{E*} = RT \ln a_{Si}^* - RT \ln(Y^* Z^* - Y^* Z^* W^*) = \sum_{j=2}^j \sum_{k=0}^{k'} \frac{A_{jk0}}{j-1} + \sum_{j=2}^j \sum_{k=0}^{k'} \sum_{l=0}^{l'} A_{jkl} Y^{*j} Z^{*k} W^{*l} + \sum_{j=2}^j \sum_{k=0}^{k'} \sum_{l=0}^{l'} A_{jkl} Y^{*j} Z^{*k} W^{*l} \left[ \frac{j-k}{Y^*(1-j)} + \frac{k-l}{Y^* Z^*(1-j)} \right] \quad (16)$$

where, asterisks in Eq(15) and (16) denote the composition variables and the activities in the coexistence line.

The simultaneous solution of Eq(13)-Eq(16) defines the  $A_{jkl}$  parameters. The solution has done by following least-square fitting procedure:

$$\varepsilon^2 = \sum_{j=1}^n w_j (\text{opt} \Delta G_i^E - \text{obs} \Delta G_i^E)^2 \rightarrow \min \quad (17)$$

(i=C, Mn, Si, Fe j = 1,2,...,n)

where,  $\varepsilon$  is the fitting errors,  $w_j$  is the fitting wights, and  $n$  is the number of samples.

For predicting the activities in the whole homogeneity of C-Mn-Si-Fe quaternary melts precisely and efficiently, the  $A_{jkl}$  parameters represented the properties of sub-ternaries and sub-binaries should be evaluated at first<sup>[1]</sup>.

For the C-Mn(1-2) sub-binary system, silicon and iron are not existed ( $Z=0$  and  $W=0$ ). Substituting these two relations into Eq(2), then the excess partial Gibbs energy of Mn may rewritten as,

$$\Delta G_{Mn(C-Mn)}^E = \sum_{j=2}^j \frac{A_{j00}}{j-1} + \sum_{j=2}^j A_{j00} Y^j \left[ 1 + \frac{j-k}{Y(1-j)} \right] \quad (18)$$

Setting the upper limits of the summation  $j'=4$ , based on the experiment results of  $\Delta G_{Mn(C-Mn)}^E$  at 1623K<sup>[6]</sup> and 1800K<sup>[7]</sup>, three  $A_{j00}$  ( $j=2,3,4$ ) binary parameters have been fitted by means of least-square techniques.  $\Delta G_{Mn(C-Mn)}^E$  were corrected previously to 1873K with the aid of Gibbs-Helmholz equation. For other sub-binary systems, parameter evaluation procedures are similar to that of in C-Mn binary. Detail information is listed in Table 1.

Next is an example to show the ternary parameter evaluation procedure. As Figure 1 illustrated, the thermodynamic relation of  $C_{\text{sat}}$ -Mn-Si alloys is similar to  $C_{\text{sat}}$ -Mn-Si-Fe quaternary ones. So, the thermodynamic relations described by Eq(13) through Eq(16) are still hold in this ternary melts. Substituting the degeneration condition ( $W=0$ ) and three group of binary parameters into Eq(13), rearrangement yields,

$$\sum_{j=2}^j A_{j00} Y^j + \sum_{j=2}^j (A_j^{13} - A_{j00}) Y^j Z + \sum_{k=2}^{k'} \frac{A_k^{23}}{k-1} Y^2 (Z^k - Z) + \sum_{j=3}^j \sum_{k=2}^{k'} A_{jkl} \left( Y^j + \frac{Y^2}{1-j} \right) (Z^k - Z) = -RT \ln(1 - Y) \quad (19)$$

Eq(14) through Eq(16) may be rearranged in the way similar to that of Eq(13). Let  $j'=k'=4$ ,  $j'+k'=7$ , solving Eq(13) through Eq(16) simultaneously, 5 ternary parameters  $A_{jkl}$  ( $j \geq 3, k \geq 2$ ) of C-Mn-Si system have been obtained on the carbon solubility data. The remains parameters can be calculated according to the formulas listed in Table 1.

Similar to C-Mn-Si alloy, ternary parameters  $A_{jl}^{134}$  for C-Si-Fe sub-ternary system have been evaluated on the carbon solubility of Si-Fe alloys and three group of binary parameters.

The solubility of carbon in Mn-Fe alloys were reported in the literature<sup>[9,10]</sup>. Graphite is the only stable phase in equilibrium with  $C_{\text{sat}}$ -Mn-Fe alloys at 1873K. Activities of manganese in Mn-Si-Fe alloys at 1700K were reported by Gee and Rosenqvist<sup>[7]</sup>. In this work, measured  $a_{\text{Mn}}$  in Mn-Si-Fe alloys were corrected to 1873K with the relations between manganese vapor pressure and temperature<sup>[7]</sup>. Therefore, ternary parameters  $A_{jl}^{124}$  and  $A_{kl}^{234}$  for C-Mn-Fe and Mn-Si-Fe alloys can be fitted just following Eq(19). Table 2. shows the detail information of four sub-ternaries used in this article.

Since the binary and ternary parameters have been evaluated, the parameters  $A_{jkl}$  ( $j \geq 3, k \geq 2, l \geq 2$ ) that indicates the quaternary system information can be evaluated along the carbon solubility data of C-Mn-Si-Fe melts. Let  $j'+k'+l'=9$ , nine of quaternary parameters have been fitted by solving Eq(13) through Eq(16) simultaneously. The rest quaternary parameters can be determined according to formulas listed in Table 2. All the parameters of C-Mn-Si-Fe quaternary liquid alloys are listed in Table 3.

Table 2. The Boundary Conditions in Ternary Systems

Ternary	Property and Resource	Evaluated Parameters	Reference
C-Mn-Si(1-2-3)	Carbon solubility of Mn-Si alloys at 1873K, $A_{j00}$ , $A_j^{13}$ , $A_k^{23}$ and $a_C^*$ , $a_{Si}^*$	$A_{jk}^{123} = A_{jkl}$	[5]
C-Mn-Fe(1-2-4)	Carbon solubility of C-Mn-Fe alloys at 1873K, $A_{j00}$ , $A_j^{14}$ and $A_k^{24}$	$A_{jk}^{124} = \sum_{l=0}^{l'} A_{jkl}$	[15]
C-Si-Fe(1-3-4)	Carbon solubility of C-Si-Fe alloys at 1873K, $A_j^{13}$ , $A_i^{34}$ and $a_C^*$ , $a_{Si}^*$	$A_{jl}^{134} = \sum_{k=0}^{k'} A_{jkl}$	[4]
Mn-Si-Fe(2-3-4)	$\Delta G_{Mn(Mn-Si-Fe)}^E$ at 1700K, $A_k^{23}$ , $A_k^{24}$ and $A_i^{34}$	$A_{kl}^{234} = \sum_{j=2}^j A_{jkl} \frac{k-1}{j-1}$	[7]

Table 3. The  $A_{jkl}$  Parameters for C-Mn-Si-Fe Quaternary Alloy at 1873K (J/mol)

		l = 0	l = 1	l = 2	l = 3	l = 4
j = 2	k = 0	515766.7	0	0	0	0
	k = 1	-43590.46	-72270.11	-1339763	2195663	-1014416
	k = 2	-179439.6	1432170	-1704778	-186386.9	626487
	k = 3	-1126557	1327537	1477688	-1957427	310313.8
	k = 4	1168272	-2726285	1521124	19900.67	0
j = 3	k = 0	-1064194	0	0	0	0
	k = 1	135276	-187364.6	5820447	-7037003	2028831
	k = 2	1923129	-7098337	4241677	2898268	-1937368
	k = 3	866079.3	928634.8	-5056720	3226083	0
	k = 4	-2226392	5567517	-3314780	0	0
j = 4	k = 0	549825.9	0	0	0	0
	k = 1	215307.8	32502.07	-4711383	3968515	-2141671
	k = 2	-2722537	7185412	-1604358	-2863604	0
	k = 3	1953612	-5834647	3864031	0	0

4. Calculation Results And Discussion

Figure 2 is the calculation results of component activities in  $C_{sat}$ -Mn-Si-Fe alloys at 1873K with Mn/Fe ratio varies from 2 to 4. From this diagram we can conclude that increase of Mn/Fe ratio in  $C_{sat}$ -Mn-Si-Fe alloys (with same silicon content) will result in increased activities of manganese and decreased activities of silicon. Calculated silicon activities in graphite/SiC/alloy co-existence line illustrate a good agreement with the experimental ones.

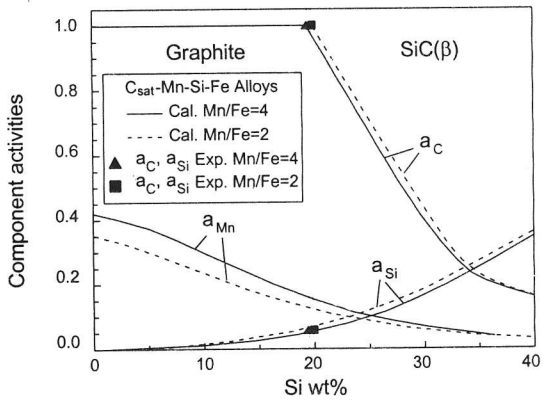


Figure 2. Component activities in  $C_{sat}$ -Mn-Si-Fe alloy with various Mn/Fe ratio at 1873K

Figure 3 shows the predicted iso-activity curves of C, Mn and Si in C-Mn-Si-Fe(Mn/Fe=4) alloys at 1873K. Because of the problem of finding suitable crucible in laboratory measurement, Si distribution equilibria between carbon unsaturated manganese alloy and slag is not available directly from experiment. Therefore, the calculation results presented in Figure 3 is very useful to predict the element distribution equilibria between carbon unsaturated C-Mn-Si-Fe alloys and relevant slags. Application of these calculation results will be discussed in later.

Since the silicon activities in  $C_{sat}$ -Si-Fe and  $C_{sat}$ -Mn-Si alloys were measured in laboratory, we can use them to check the calculation results. The effect of carbon and silicon on the activity of silicon in  $C_{sat}$ -Si-Fe alloys was studied by Chipman *et al.*<sup>[12]</sup>. They found the contribution of  $X_C+X_{Si}$  towards the activity of silicon to be

approximately the same as that of  $X_{Si}$  for Si-Fe binary alloys. A similar observation was made by Gee *et al.*<sup>[7]</sup> and one of the author<sup>[5]</sup> in  $C_{sat}$ -Mn-Si alloys. In Figure 4, calculated  $a_{Si}$  of  $C_{sat}$ -Mn-Si alloys as a function of  $X_C+X_{Si}$  almost overlaps the curves of  $a_{Si}$  in Mn-Si binary alloys vs  $X_{Si}$ . This figure is a good example to prove correctness of the present calculation.

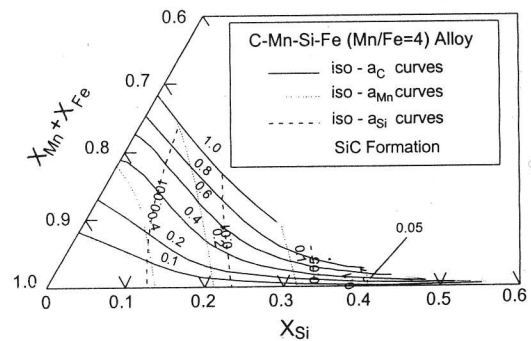


Figure 3. Iso-activity curves of C-Mn-Si-Fe quaternary alloys with Mn/Fe=4 at 1873K

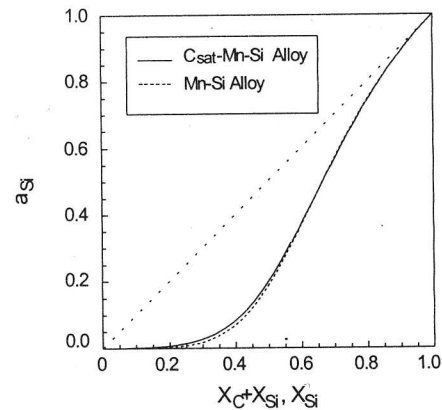
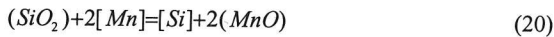


Figure 4. A comparison of  $a_{Si}$  between Si-Mn and  $C_{sat}$ -Mn-Si alloy at 1873K

Slag/alloy distribution equilibria are of theoretical as well as of

practical interest. One of the author conducted dozens of equilibrium experiments<sup>[5,6]</sup>. A comprehensive knowledge of silicon and manganese distribution equilibria between  $C_{sat}$ -Mn-Si ternary alloys and  $MnO-SiO_2-CaO-Al_2O_3$  slags were established in laboratory. The reaction equilibria between C-Mn-Si-Fe quaternary alloys and  $MnO-SiO_2-CaO-Al_2O_3$  slags can be predicted qualitatively by combination of the experiment results and the calculated thermodynamic properties of C-Mn-Si-Fe alloys.

The reactions taken into account to evaluated equilibrium conditions in slag/alloy equilibria is mainly depended on:



If the reaction achieves equilibrium, following regulation must be satisfied,

$$\frac{a_{Mn}^2}{a_{Si}} = K \cdot \frac{a_{MnO}^2}{a_{SiO_2}} \quad (21)$$

where,  $K$  is the equilibrium constant of the above reaction.

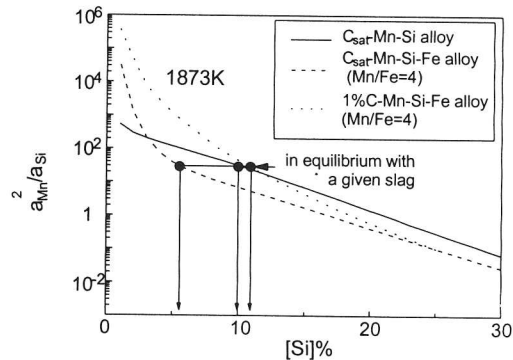


Fig. 5 Activity ratio  $a_{Mn}^2/a_{Si}$  as a function of Silicon content with deferent alloys

Calculated activity ratio vs silicon content in different manganese alloys at 1873K are showed in Figure 5. According to the curves shown in Figure 5, carbon content in manganese alloys changes remarkably the equilibrium composition of silicon in metal phase. Carbon unsaturated alloys will contain more silicon than carbon saturated alloys suppose being in equilibrium with the same slag. Silicon composition will increase if the alloy is decarbonized in equilibrium with a given slag. Addition of iron to manganese alloys will bring a complicated influence over the silicon distribution between alloys and slags. At the high Si content range, iron also reduces the activity ration  $a_{Mn}^2/a_{Si}$  both in carbon saturated and unsaturated alloys. As a consequence, Si content decreases with increasing iron content for alloys in equilibrium with the same slag. At the lower silicon content range, however, addition of iron to Mn-Si-C alloys will increase the Si concentration. A similar observation was found by Ding<sup>[5]</sup>. He found that the Si content in  $C_{sat}$ -Mn-Si-15%Fe alloy equilibrated with silica-saturated  $MnO-SiO_2$  binary slag is about 0.8% higher than in

the  $C_{sat}$ -Mn-Si alloy at 1823K. At MnO-saturation range, the equilibrium silicon concentration in quaternary alloy is approximately 0.5% lower then in the iron-free alloy.

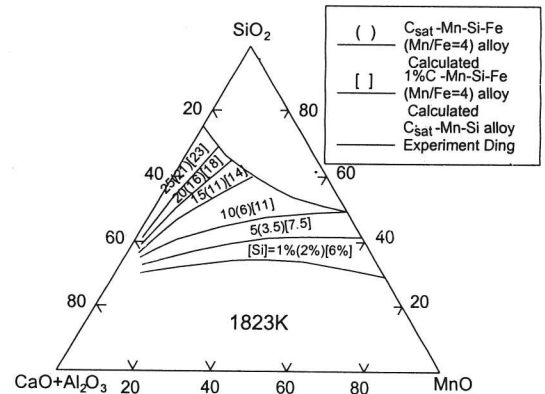


Figure 6. Equilibrium relations in quaternary  $MnO-SiO_2-CaO-Al_2O_3$  ( $CaO/Al_2O_3=3$ )slags in contact with manganese alloys

The silicon distribution between quaternary alloys and  $MnO-SiO_2-CaO-Al_2O_3$  slags can be easily predicted by integrating the equilibrium experiment results and the calculated activity ratio of different alloys illustrated in Figure 5. The resulting of silicon distribution between  $C_{sat}$ -Mn-Si-Fe(Mn/Fe=4) alloys and  $MnO-SiO_2-CaO-Al_2O_3$  ( $C/A=3$ ) slags is shown in Figure 6. Silicon distribution equilibria between 1%C-Mn-Si-Fe(Mn/Fe=4) alloys and  $MnO-SiO_2-CaO$  ternary slags at 1823K is also presented in this diagram. These diagrams can be used as a tool to optimize the processes.

### 5. Conclusion

Based on the carbon solubility of Mn-Si-Fe alloy and the boundary conditions in its sub-binary and sub-ternary systems, component activities of C-Mn-Si-Fe liquid alloys have been predicted with aid of the new solution model. The calculation results are examined by the experimental data. The equilibrium relations associated with the production of manganese ferroalloys are also calculated in the present paper.

### Reference

1. Tang K., Dr. Thesis, "Study on Subregular Solution Model SELF-SReM4.1 for Multicomponent System and the Application to Analyzing Metallurgical Processes", Shanghai University, 1997.12. China
2. M.S.Petrushevskii, and V.P.Gel'd , "Equilibrium of Carbon with Liquid Alloys of Fe, Mn, Si and C", Journal of Applied Chemistry of USSR, 32(1959), 86
3. J.Kr.Tuset, and J.Sandvik, SINTEF Research Report 340358, 1970, 33
4. J.Chipman, J.C.Fulton, N.Gockcen, and G.R.Caskey, "Activity of Silicon in Liquid Fe-Si and Fe-C-Si Alloys", Acta Met, 2(1954), 439-450
5. W.Z.Ding, Dr. Thesis, "Equilibrium Relations in the Production of Manganese Alloys", Trondheim, Norway, 1993.1.

6. W.Z.Ding, and Olsen S E, "Reaction Equilibria in the Production of Manganese Ferroalloys", Metallurgical and Materials Trans. 27B(1996), 5-17
7. R.Gee, and T.Rosenqvist, "The Vapour Pressure of Liquid Manganese and Activities in Liquid Mn-Si and Carbon-saturated Mn-Si Alloys", Scandinavian J. Metall. 5(1976), 57-62
8. A.Katsnelson, F.Tsukihashi, and N.Sano, ISIJ Int., 33(1993)10, 1045
9. R.Hultgren, P.D.Desai, D.T.Hawkins, M.Gleiser, and K.K. Kelley, "Selected Values of the Thermodynamic Properties of Binary Alloy", Metal Park, Ohio, AIME, 1973
10. E.T.Turkdogan, R.A.Hancock, and S.I.Herlize, "The Solubility of Graphite in Manganese, Cobalt and Nickel", JISI, 182(1956), 274-277
11. A.Tanaka, "Determination of the Activities in Mn-C and Mn-Si Melts by Vapor Pressure Measure", Trans JIM, 20(1979), 516-552
12. J.Chipman, and R.Baschwitz, Trans Met. Soc. AIME., 227(1963), 473-478